

Micromachined CPW-Fed Suspended Patch Antenna For 77 GHz Automotive Radar Applications

Hyung Suk Lee, Jeong-Geun Kim, Songcheol Hong, Jun-Bo Yoon

Korea Advanced Institute of Science and Technology, Department of Electrical Engineering and Computer Science, Daejeon 305-701, Korea (e-mail: hslee@3dmems.kaist.ac.kr)

Abstract — A new approach to high performance patch antenna at millimeter wave, especially 77 GHz of frequency for automotive applications, is introduced. The proposed antenna is composed of coplanar waveguide (CPW) feed line, a feeding post, supporting posts, and a radiating patch. The performance of antenna was improved by elevating the radiating patch in the air while remaining feed network on the high dielectric constant substrate. A 2×1 array antenna was also designed with a simple feed network. The fabricated antenna showed broadband characteristics and high radiation efficiency. Measured -10 dB bandwidths were about 9.0 GHz (11.8 %) from 73.3 GHz to 82.3 GHz in single patch antenna and about 10.0 GHz (12.7 %) from 73.9 GHz to 83.9 GHz in 2×1 patch array antenna. Simulated radiation efficiencies were 94 % for single patch antenna and 93 % for 2×1 patch array antenna respectively.

I. INTRODUCTION

Safe driving support technology is an important field in development for intelligent transport systems (ITS). Especially, 77 GHz automotive radar front-end is a key component of adaptive cruise control (ACC) systems [1]. In the radar front-end, antenna is one of key components which determine the performances of radar system. To increase the detection range and resolution, the antenna with high gain and broad bandwidth is strongly required. Furthermore, because antenna is one of the largest components in the radar front-end, reducing antenna size is increasingly important to make compact radar systems [2], [3]. At mm-wave frequency such as 77 GHz for automotive radar applications, horn antenna is usually used due to its high performance, but it is very bulky, heavy, and high costly. Moreover, the transition such as waveguide-to-microstrip transition has to be needed to interconnect with monolithic microwave integrated circuits (MMICs). On the other hand, patch antennas have been a common choice for integrated antennas because they are low profile, simple, and low costly. However, patch antennas also have major operational disadvantages at mm-wave such as narrow bandwidth and low gain due to their inherent low efficiency. So they can not be applied well at mm-wave frequency.

Compact size and high performance can be achieved by integrating the patch antenna on the low dielectric constant material with thick thickness while remaining the circuitry on the high dielectric constant regions in the same substrate. Recently as the micromachining technology is developed, it is applied to the antenna to improve the antenna performance. In order to reduce effective dielectric constant of substrate under the patch

antenna, various methods have been reported such as making a cavity around and beneath the patch antenna using the bulk micromachining, stacking substrates and coupling through aperture, and suspending the patch antenna over an air cavity using a membrane, etc. [4]-[6]. These all researches were achieved high performances compared to conventional printed patch antennas on the relatively high dielectric constant substrate. However, the process such as etching the substrate and fabricating the membrane is very tricky. Also, when they fabricated as array, complex feed line such as $1/4 \lambda$ impedance transformer leads an unwanted radiation.

In this paper, a CPW-fed suspended patch antenna with high performance using the surface micromachining technology at mm-wave frequency of 77 GHz is investigated.

II. DESIGN OF CPW-FED SUSPENDED PATCH ANTENNA

Fig. 1 shows the perspective view of the proposed antenna structure, which is composed of CPW feed line, a feeding post, two additional supporting posts, and a radiating patch. In the proposed antenna, two additional supporting posts are optional to support the radiating patch more robustly. The CPW line used as signal feed line shows better performances such as lower radiation loss and weaker crosstalk effects than a microstrip line at mm-wave frequency. The CPW line has the uniplanar construction which implies that all of the signal lines and ground planes are on the same surface of the substrate. This attribute simplifies manufacturing by eliminating the need for backside via holes and substrate lapping [7], [8]. Furthermore, the ground plane of CPW line can be used as the ground plane of the radiating patch when the radiating patch is supported with the feeding post like a coaxial probe feeding method. Therefore, the CPW feed line can be placed on the substrate of high dielectric constant, but the radiating patch is formed on the air as shown in Fig. 1.

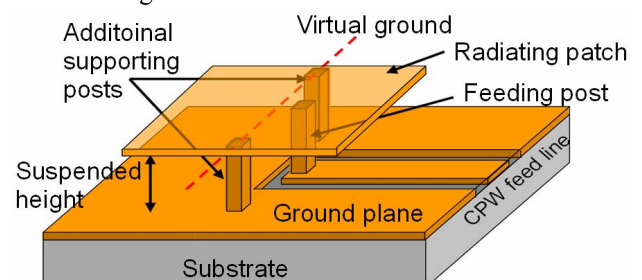


Fig. 1. Illustration of the proposed antenna structure. Additional supporting posts are optional for the robustness.

Because the radiating patch is supported with metal posts on the air, there are no dielectric losses and thus the performance of antenna can be improved. The proposed antenna has a feeding post which functions as a signal line and a supporter of the radiating patch simultaneously. An appropriate input impedance of the proposed patch antenna can be selected by just locating feeding post as the same method as the coaxial probe feeding, thus the antenna can be directly matched to various input impedances [9]. Besides the feeding post for the signal line, there are two additional supporting posts for robust structure. Because these two additional supporting posts are placed at virtual ground of the radiating patch and connected to the ground plane of CPW, the additional supporting posts do not affect the performance of antenna.

In order to decide appropriate height of suspended patch antenna and optimum design, pre-simulations were performed by using 2.5-dimensional electromagnetic (EM) simulator of Ansoft Designer and 3-dimensional EM simulator of CST Microwave Studio 5.0. Besides the proposed antenna with various heights, a conventional printed edge-fed microstrip patch antenna on 100 μm -thick Duroid substrate which has the dielectric constant of 2.2 and the loss tangent of 0.001 were simulated to compare the performances of proposed antenna with those of conventional printed patch antenna.

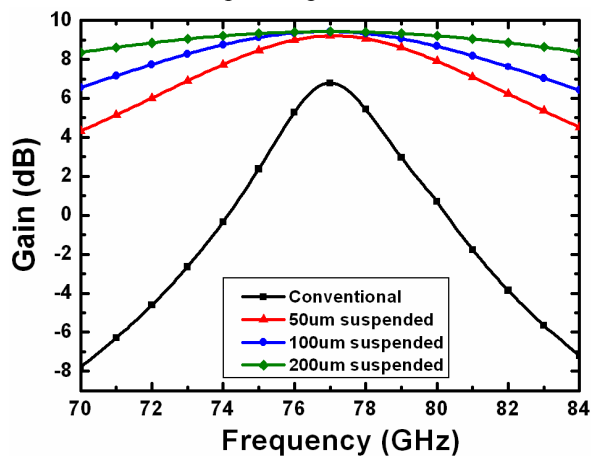


Fig. 2. Simulation result of gain for conventional printed patch antenna and proposed antenna with various suspended heights.

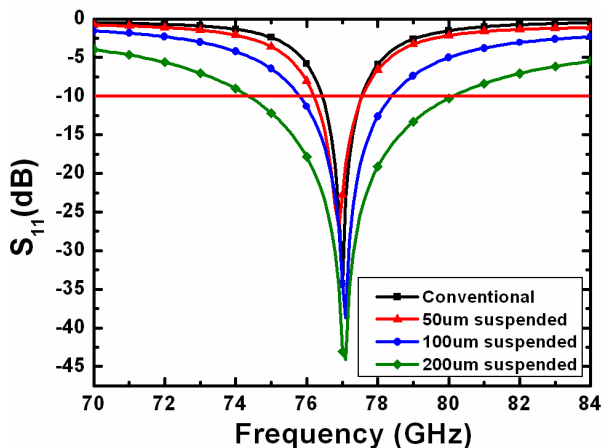


Fig. 3. Simulation result of input return loss for conventional printed patch antenna and proposed antenna with various suspended heights.

Fig. 2 and Fig. 3 show the simulation results for the gain and the input return loss. As shown in Fig. 2, the gain of proposed antenna was 3 dB higher than that of conventional printed patch antenna regardless of suspended height. In Fig. 3, the -10 dB bandwidth was also improved to twice as the height becomes twice. Most desirable substrates for antenna performance are thicker substrate whose dielectric constant is in the lower end of the range, e.g. air.

2×1 patch array antenna was also designed as well as single patch antenna. Two patches were separated with the distance of about 0.8λ in which the antenna shows high gain property. Fig. 4 shows the designed 2×1 patch array antenna. The input impedance of each patch was selected to 100 Ω to design without $1/4 \lambda$ impedance transformer. Two patches were fed with 100 Ω CPW line and then two 100 Ω CPW lines were combined with 50 Ω CPW line directly. Because there is no $1/4 \lambda$ impedance transformer which is required in edge-feed patch antenna, the patch array antenna can be designed simply and minimized the discontinuities of the feed line which occur the unwanted radiation.

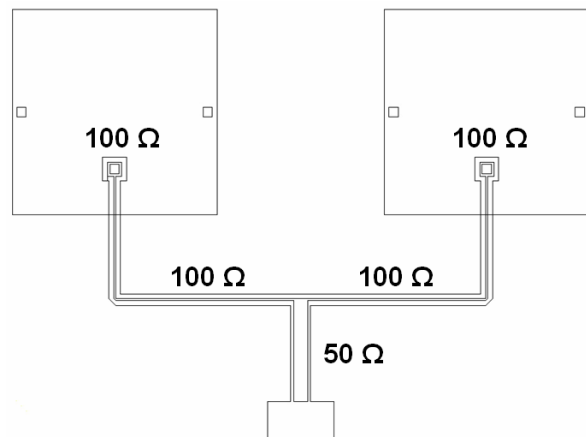


Fig. 4. Design layout of 2×1 patch array antenna.

III. FABRICATION OF THE ANTENNA

CPW-fed suspended patch antenna with the height of 200 μm air suspension was fabricated on the glass substrate using the surface micromachining technology. For the glass substrate, Corning Pyrex 7740 which had the dielectric constant of 4.6 and substrate thickness of 800 μm was used.

To build up highly suspended structure, two elementary key processes were used and set up. One is thick photoresist lithography process and the other is thick metal electroplating process. Fig. 5 shows the fabrication process steps. At first, Ti (200 \AA)/Cu (2000 \AA) metal seed layer was deposited by thermal evaporation (Fig. 5(a)). For the formation of CPW feed line, conventional lithography with thick positive photoresist followed by Cu electroplating was done (Fig. 5(b)). For photoresist lithography process, AZ 9260 positive photoresist was used because this photoresist gives a reliable fine pattern around several tens micron order of photoresist thickness. In thick metal electroplating process, the key effort is the control of current density because the current density determines

the growth rate of electroplating and the uniformity of electroplated Cu surface. The best choice of current density is $10\sim 20\text{ mA/cm}^2$ for the uniform surface.

After removing the photoresist of AZ 9260, the posts to flow signals and support the radiating patch were formed through two steps (Fig. 5(c) and Fig. 5(d)). In these steps, thick negative photoresist of THB-151NTM and Cu electroplating were utilized. For fine pattern of post with $200\ \mu\text{m}$ height, two repeated steps were performed, that is, $100\ \mu\text{m}$ -high post was formed and next $100\ \mu\text{m}$ -high post was formed again. After the post was formed, the top seed metal of $500\ \text{\AA}$ -thick Cu was evaporated to form the radiating patch (Fig. 5(e)). The next step is the formation of radiating patch (Fig. 5(f)). The positive photoresist, AZ 9260, was patterned and Cu electroplating of $10\ \mu\text{m}$ thickness was done. For the radiating patch, lusterless Cu electroplating was done to prevent bending the radiating patch. In general, the lusterless Cu electroplating has less stress than luster Cu electroplating.

The last two steps are stripping and etching of all sacrificial layers except antenna structure. The positive photoresist patterned to form the radiating patch was developed and the top Cu seed was etched away using the Cu seed etchant (Fig. 5(g)). Finally, THB-151NTM negative photoresist was stripped and bottom Ti/Cu seed was etched away for electrical isolation between devices (Fig. 5(h)). Then proposed CPW-fed suspended patch antenna supported by post with the height of $200\ \mu\text{m}$ was completely fabricated.

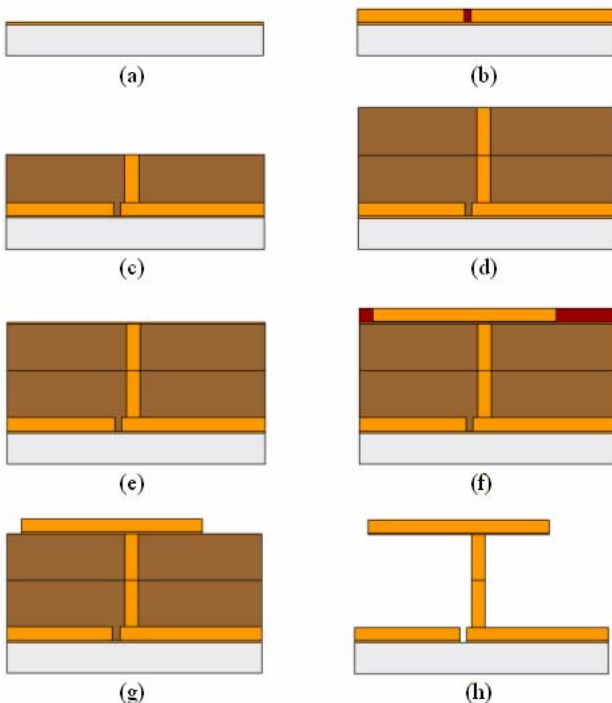


Fig. 5. Fabrication process steps. (a) Thermal evaporation of Ti/Cu seed layer. (b) $10\ \mu\text{m}$ -thick positive photoresist patterning followed by Cu electroplating. (c) $100\ \mu\text{m}$ -thick negative photoresist patterning followed by Cu electroplating. (d) Repeat step (c). (e) Thermal evaporation of Cu seed layer. (f) $10\ \mu\text{m}$ -thick positive photoresist patterning followed by lusterless Cu electroplating. (g) Strip positive photoresist and etch Cu seed layer. (h) Strip negative photoresist and etch Ti/Cu seed layer.

Single patch antennas with and without additional supporting posts and 2×1 patch array antenna with additional supporting posts were fabricated. In practice, additional supporting posts offered better producibility on manufacturing the array structure.

The SEM photographs of the fabricated antenna are shown in Fig. 6. Fig. 6(a) shows the cross sectional view of single patch antenna without additional supporting posts. Fig. 6(b) shows the perspective view and cross sectional view (small photograph) of 2×1 patch array antenna with additional supporting posts. The size of each radiating patch is $1.7\ \text{mm} \times 1.7\ \text{mm}$ and the suspended height is $200\ \mu\text{m}$.

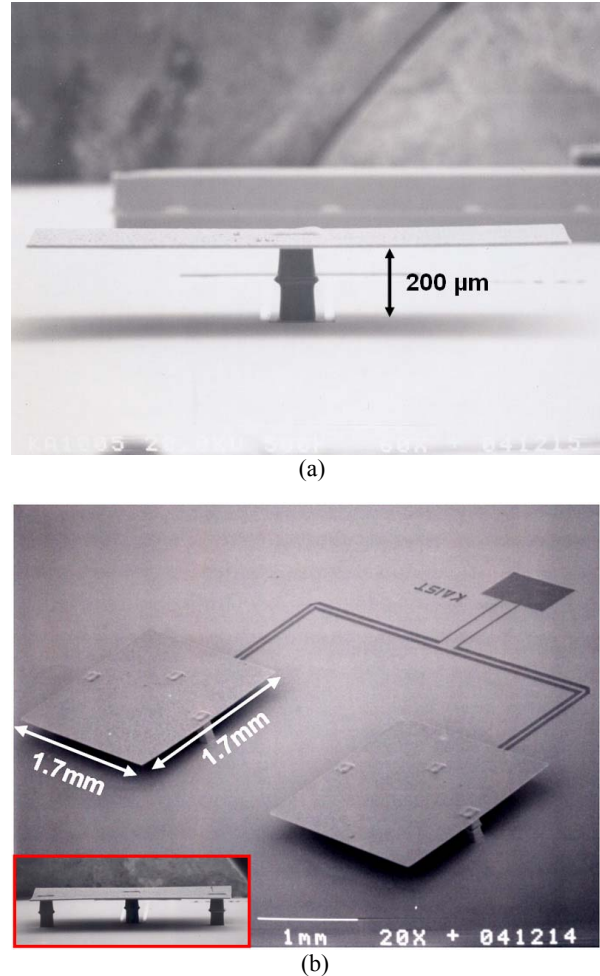


Fig. 6. SEM photographs of the fabricated antenna. (a) The cross sectional view of single patch antenna without additional supporting posts. (b) The perspective view and cross sectional view of 2×1 patch array antenna with additional supporting posts.

IV. MEASUREMENT RESULT

Input return losses of fabricated antennas and array antennas were measured by using Anritsu broadband vector network analyzer of ME7808A. All measurements were performed on-wafer measurement on Karl Suss probe station.

Fig. 7 shows the simulated and measured results of input return loss for the fabricated single patch antenna without additional supporting posts. Measured $-10\ \text{dB}$

bandwidth was about 9.0 GHz (11.8 %) from 73.3 GHz to 82.3 GHz.

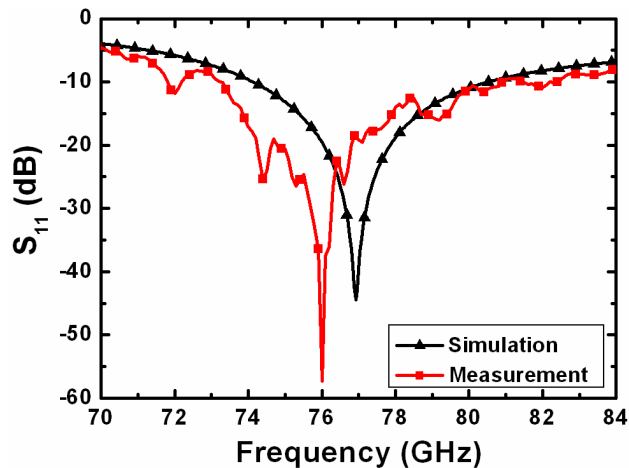


Fig. 7. Simulated and measured results of input return loss for the fabricated single patch antenna without additional supporting posts.

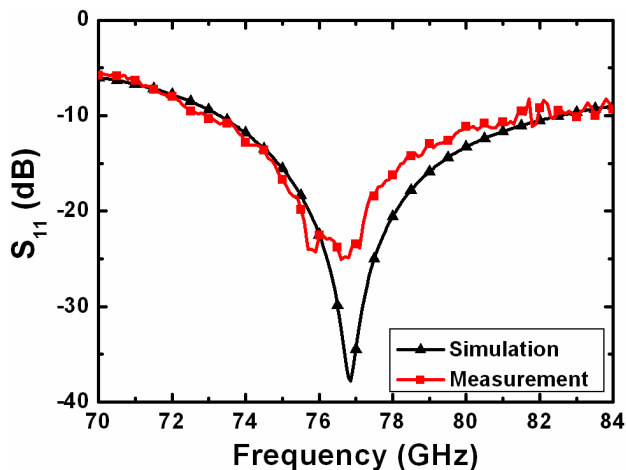


Fig. 8. Simulated and measured results of input return loss for the fabricated single patch antenna with additional supporting posts.

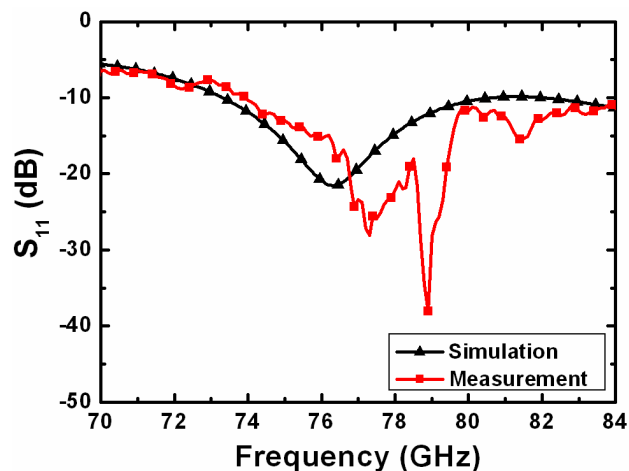


Fig. 9. Simulated and measured results of input return loss for the fabricated 2×1 patch array antenna with additional supporting posts.

In case of the single patch antenna with additional supporting posts, the simulated and measured results of input return loss are shown in Fig. 8. Measured -10 dB bandwidth was about 8.5 GHz (11.0 %) from 72.9 GHz to 81.4 GHz. From the results of Fig. 7 and Fig. 8, the effect of additional supporting posts to the electric performances of antenna is negligible.

Fig. 9 shows the simulated and measured results of input return loss for 2×1 patch array antenna with additional supporting posts. Measured -10 dB bandwidth was about 10.0 GHz (12.7 %) from 73.9 GHz to 83.9 GHz. All the measurement results agreed well with the simulated results.

V. CONCLUSION

CPW-fed suspended patch antenna at 77 GHz for automotive radar applications was designed and fabricated using the surface micromachining technology. Presented antenna was designed to suspend 200 μm -high in the air from CPW feed line. This suspended structure gives the freedom of selecting substrate under the CPW feed line. The fabricated antenna has shown good performances. We believe that the proposed antenna can allow the freedom of process in the current printed patch antenna technology. Moreover, because the proposed antenna is easily integrated with MMICs, it can be applied to radar on a chip (ROC) including the antenna at mm-wave frequency.

REFERENCES

- [1] F. Gallée, G. Landrac and M.M. Ney, "Artificial lens for third-generation automotive radar antenna at millimeter-wave frequencies," *IEEE Proceedings of Microwaves, Antennas and Propagation*, vol. 150, no. 6, Dec. 2003, pp. 470-476.
- [2] S.W. Alland, "Antenna requirements for automotive radar antenna," *Proceedings of the 1998 IEEE Radar Conference*, Dallas, USA, May 1998, pp. 367-372.
- [3] E.G. Hoare, and R. Hill, "System requirements for automotive radar antennas," *IEE Colloquium on Antennas for Automotives*, London, UK, Oct. 2000, pp. 1-11.
- [4] J.P. Papapolymerou, R.F. Drayton, and L.P.B. Katehi, "Micromachined patch antennas," *IEEE Transactions on Antennas and Propagation*, vol. 46, pp. 275-283, Feb. 1998.
- [5] G.P. Gauthier, A. Courtauy, and G.M. Rebeiz, "Microstrip antennas on synthesized low dielectric-constant substrates," *IEEE Transactions on Antennas and Propagation*, vol. 45, pp. 1310-1314, Aug. 1997.
- [6] G.P. Gauthier, J.P. Raskinn, and L.P.B. Katehi, "A 94-GHz aperture-coupled micromachined microstrip antenna," *IEEE Transactions on Antennas and Propagation*, vol. 47, pp. 1761-1766, Dec. 1999.
- [7] K.J. Herrick, T.A. Schwarz, and L.P.B. Katehi, "Sim-machined coplanar waveguides for use in high-frequency circuits," *IEEE Transactions on Microwave Theory and Techniques*, vol. 46, pp. 762-768, June 1998.
- [8] C. Schollhorn, Z. Weiwei, M. Morschbach, and E. Kasper, "Attenuation mechanisms of aluminum millimeter-wave coplanar waveguides on silicon," *IEEE Transactions on Electron Devices*, vol. 50, pp. 740-746, Mar. 2003.
- [9] R. Grag, P. Bhartia, I. Bahl, and A. Ittipiboon, *Microstrip Antenna Design Handbook*, Artech House, 2000.